#### **PROCEEDINGS A**

royalsocietypublishing.org/journal/rspa

# Research



**Cite this article:** Adili A, Chen Y, Lipton R, Walker S. 2022 Controlling the dispersion of metamaterials in three dimensions. *Proc. R. Soc. A* **478**: 20220194. https://doi.org/10.1098/rspa.2022.0194

Received: 18 March 2022 Accepted: 14 June 2022

# Subject Areas:

applied mathematics

#### **Keywords:**

power series, homogenization, subwavelength resonance, Maxwell's equations, metmaterial crystals

#### **Author for correspondence:**

Abiti Adili

e-mail: abiti\_adili@uml.edu

# Controlling the dispersion of metamaterials in three dimensions

Abiti Adili<sup>1</sup>, Yue Chen<sup>2</sup>, Robert Lipton<sup>3</sup> and Shawn Walker<sup>3</sup>

<sup>1</sup>Department of Mathematical Sciences, University of Massachusetts Lowell, Lowell, MA 01854, USA

<sup>2</sup>Department of Mathematics, Auburn University at Montgomery, Montgomery, AL 36117, USA

<sup>3</sup>Department of Mathematics, Louisiana State University, Baton Rouge, LA 70803, USA

AA, 0000-0001-6451-6960; YC, 0000-0003-1724-5197; RL, 0000-0002-1382-3204; SW, 0000-0002-8027-5789

We provide a platform to examine the effect inclusion geometry on three-dimensional metamaterial crystals to tune frequency-dependent effective properties for control of leading order dispersive behaviour. The crystal is non-magnetic and made from all dielectric components. The design provides novel dispersive properties using subwavelength resonances controlled by the geometry of the media. We numerically calculate the effective tensors of the metamaterial to identify frequency intervals where the metamaterial exhibits band gaps as well as intervals of normal dispersion and double negative dispersion. The frequency intervals can be explicitly controlled by adjusting the geometry and placement of the dielectric inclusions within the period cell of the crystal.

# 1. Introduction and problem set-up

# (a) Introduction

Metamaterials exhibit novel properties not found in nature. These properties are generated by periodically patterned composite material crystals. When the period of the crystal is less than the wavelength of incident radiation, interesting interactions occur between the material and the electromagnetic waves. This provides the opportunity for manipulation of structural geometry

to obtain novel dispersive properties. One such property is exhibited by the double negative metamaterial which has frequency-dependent negative effective magnetic permeability and negative effective dielectric permittivity. Metamaterials with double negative effective properties have a wide range of applications ranging from biomedical imaging to optical lithography and data storage. In 1968, the novel properties of materials were studied under the assumption of negative dielectric constant and negative magnetic permeability [1]. The double negative effective properties of a periodic array of non-magnetic metallic split-ring resonators at microwave frequency were studied in [2]. The double negative properties of metamaterials made from arrays of metallic posts and split-ring resonators were experimentally demonstrated in [3]. Double negative properties of materials were obtained for metallic resonators with different geometric structures in [4–9]. Negative refractive properties of metamaterials obtained by employing dielectric material with large permittivity were studied in [10–12].

The appearance of double negative properties of metamaterials made from high dielectric core with plasmonic coating at optical frequencies was explored in [13–15]. Metamaterial crystals with double negative effective properties were obtained using periodic array of unit cells consisting of two different inclusions in [16,17]. Negative bulk dielectric permeability at infrared and optical frequencies using special configurations of plasmonic nanoparticles was studied in [18,19].

The dispersion relation and convergent power series representation for a propagating Bloch wave in a periodic medium with a single high contrast inclusion were obtained in [20–22]. The leading order terms give the effective dispersion relation of the metamaterial while the higher order terms give the corrections necessary for the diffraction due to inclusions of finite size. In the optical frequency regime, convergent power series solutions recovering dispersion relations were derived for all dielectric constituents that deliver double negative dispersive properties for transverse electric modes propagating transverse to prismatic rods [17]. For these configurations, the direction of power flow is opposite to that of phase velocity. Their frequency-dependent refractive properties were subsequently engineered in the time domain for controlling the direction of signals [23]. A setting for which the appearance of artificial magnetism for describing scattering problems for three-dimensional metamaterials using high dielectric constant inclusions was introduced and rigorously established in [24]. For three-dimensional metallic splitring geometries, the rigorous proof of effective magnetic permeability was recently given in [25]. Recently, the rigorous mathematical realization of double negative metallic media using two scale expansions for microwave frequencies was obtained in [26].

This paper analyses metamaterial crystals constructed using all dielectric materials in the near infrared-optical regime. Our choice of dielectric constituents is motivated by the work of [17]. The novelty of this work is that we focus on fully three-dimensional materials and the results are directly obtained from Maxwell's equations using power series expansions of the electromagnetic fields. The wavelength of light propagating through the periodic crystal is  $\lambda$  and the period of the crystal is d. For metamaterials, the crystal is subwavelength, i.e. the period of the structure is below the wavelength of operation, so  $2\pi d/\lambda < 1$ . We treat a non-magnetic host dielectric M impregnated with an infinite periodic array of non-magnetic inclusions with different dielectric properties. Inside any period the host material contains two types of non-magnetic included phases: one with a high dielectric constant denoted by R and the other featuring a frequency-dependent dielectric constant denoted by P. The three-dimensional period cube containing distinct inclusions of P and R is shown in figure 1 and a coated sphere geometry with core R coated with P is shown in figure 2. The leading order behaviour of the electromagnetic field inside a metamaterial made from these configurations is propagating plane waves with polarization given by averaged electric and magnetic fields. The plane waves can propagate across frequency bands determined explicitly to leading order by a dispersion relation given in terms of frequency-dependent effective magnetic permeability and permittivity. The averaged electric field is the usual average of the electric field over the period cell; however, the averaged H field is based on a geometric average over the period introduced in [24] for periodic subwavelength high dielectric materials associated with artificial magnetization; see

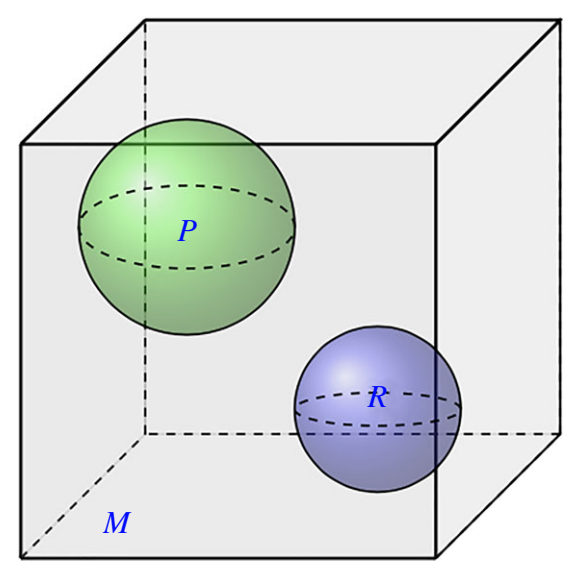
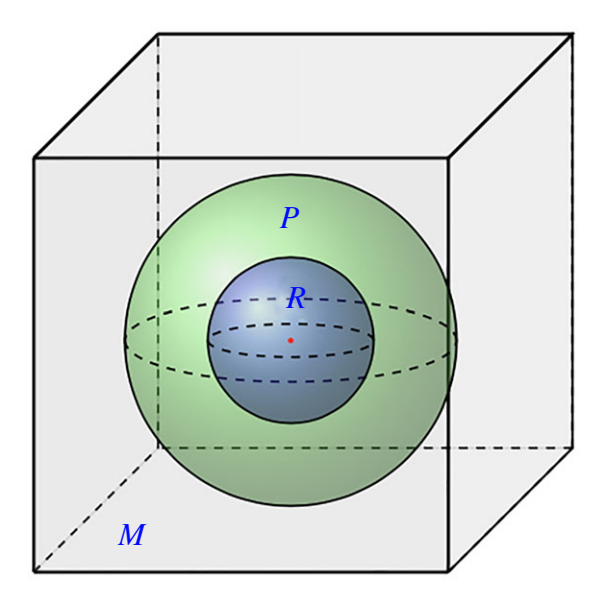


Figure 1. Period cell. (Online version in colour.)



**Figure 2.** Unit cell with a coated spherical inclusion. (Online version in colour.)

(2.8) and (2.9) of §2b. The frequency-dependent effective dielectric permittivity and magnetic permeability are described by two types of subwavelength resonances: a plasmon resonance generating frequency-dependent positive or negative effective dielectric properties and an artificial magnetic resonance generating a frequency-dependent effective magnetic permeability; see §2c. The plasomnic response of the metamaterial is due to the frequency dependence of the dielectric inclusion exciting a structural electric resonance of the electromagnetic crystal at certain frequencies. The structural resonance was calculated through generalized electrostatic resonances for periodic crystals [16,17,27]. This approach is motivated by the seminal work of [28,29] that introduces similar resonances to obtain bounds on frequency-independent effective transport properties. For dilute suspensions such resonances can be found in [30]. The magnetic

royalsocietypublishing.org/journal/rspa Proc. R. Soc. A 478: 20220194

resonances were mathematically identified and explained in the three-dimensional context in [24]; see also [31,32]. Here, we show how to employ these two resonances to rationally design double negative materials. We numerically calculate the effective properties for metamaterial crystals made from coated sphere geometries and identify frequency intervals in the optical regime where the metamaterial exhibits double negative behaviour. Here, the term double negative refers to simultaneously negative effective magnetic permeability and dielectric permittivity, implying that the propagation of energy is opposite to the direction of phase velocity. This is demonstrated in §2d.

#### (b) Problem set-up

The Maxwell system takes the form

$$\nabla \times E = -\mu_d \frac{\partial H}{\partial t},$$

$$\nabla \cdot (\varepsilon_d E) = 0,$$

$$\nabla \times H = \varepsilon_d \frac{\partial E}{\partial t}$$

$$\nabla \cdot H = 0$$
(1.1)

and

Here, E denotes the electric field and  $H = B/\mu_0$ , where B is the magnetic field. The host and inclusions are non-magnetic and  $\mu_d := \mu_0$  everywhere in the crystal where  $\mu_0$  is the free space value.

We express Maxwell's equations in terms of relative dielectric permittivity and magnetic permeability. And the dielectric constant  $\varepsilon_d(x)$  of the metamaterial crystal of period length d with period cell  $Y^d = (0, d)^3$  is given by  $\varepsilon_d = \epsilon_0 \varepsilon_{\rm rel}^d$ , where  $\epsilon_0$  is the dielectric constant in free space and the relative dielectric permittivity

$$\varepsilon_{\text{rel}}^{d} = \begin{cases} \varepsilon_{p,\text{rel}}(\omega) = 1 - \frac{\omega_{p}^{2}}{\omega^{2}} & \text{in } P, \\ \frac{\varepsilon_{r,\text{rel}}}{d^{2}} & \text{in } R, \\ 1 & \text{in } M. \end{cases}$$
(1.2)

Here,  $\varepsilon_{p,\mathrm{rel}}$  and  $\varepsilon_{r,\mathrm{rel}}$  represent the dielectric constants of the inclusions P and R, respectively, and unity is the relative dielectric constant for free space. The material characterized by  $\varepsilon_{p,\mathrm{rel}}$  is frequency dependent like gold or aluminium for near infrared and optical frequencies. To illustrate the idea,  $\varepsilon_{p,\mathrm{rel}}$  is represented by a Drude model without damping where  $\omega_p$  is the plasma frequency. The material inside inclusion R is a frequency-independent dielectric material.

We consider periodically modulated waves propagating through the crystal:

$$E(x,t) = E(x) e^{(ik\hat{k}\cdot x - i\omega t)} \quad \text{and} \quad H(x,t) = H(x) e^{(ik\hat{k}\cdot x - i\omega t)}, \tag{1.3}$$

where E(x) and H(x) are periodic,  $\hat{k}$  is the direction of wave propagation and  $|\hat{k}| = 1$ , k is the wavenumber, and  $\omega$  is the frequency. Writing

$$\mathcal{E}(x) = E(x) e^{ik\hat{k}\cdot x}$$
 and  $\mathcal{H}(x) = H(x) e^{ik\hat{k}\cdot x}$ 

and rescaling y = x/d, we have the problem posed in the unit cell  $Y = (0, 1)^3$  given by

$$\nabla \times \mathcal{E} = id\omega \mu_0 \mathcal{H}, \quad [\mathcal{H}] = 0,$$

$$\nabla \times \mathcal{H} = -id\omega \varepsilon_0 \varepsilon_{\text{rel}}^d \mathcal{E}, \quad [n \times \mathcal{E}] = 0,$$

$$\nabla \cdot \varepsilon_0 \varepsilon_{\text{rel}}^d \mathcal{E} = 0, \quad [n \cdot \varepsilon_0 \varepsilon_{\text{rel}}^d \mathcal{E}] = 0$$

$$\nabla \cdot \mathcal{H} = 0,$$

$$(1.4)$$

and

where the notation [.] indicates transmission conditions across interfaces between materials.

In this paper, power series expansion of the waves in the small parameter  $\eta = dk = 2\pi d/\lambda$  is used to investigate dispersion associated with subwavelength crystals. We expand the electric field, magnetic field and non-dimensional square frequency as

$$\mathcal{E}(y) = e_0(y) e^{i\eta \hat{k} \cdot y} + e_1(y) \eta e^{i\eta \hat{k} \cdot y} + e_2(y) \eta^2 e^{i\eta \hat{k} \cdot y} + \cdots,$$

$$\mathcal{H}(y) = h_0(y) e^{i\eta \hat{k} \cdot y} + h_1(y) \eta e^{i\eta \hat{k} \cdot y} + h_2(y) \eta^2 e^{i\eta \hat{k} \cdot y} + \cdots$$

$$\omega = \omega_0 + \omega_1 \eta + \omega_2 \eta^2 + \cdots,$$

and

where  $e_0, e_1, \ldots$  and  $h_0, h_1, \ldots$  are periodic. The expansions are substituted into (1.4) and the leading order terms  $e_0, h_0$  together with the leading order dispersion relation relating  $\omega_0$  to k are seen to describe plane wave propagation inside the metamaterial. They give the leading order behaviour for propagating electromagnetic waves inside the subwavelength medium for  $2\pi d/\lambda < 1$ .

#### 2. Main results

# (a) Characterization of leading order terms

The asymptotic analysis (see §§3b and 3e) shows that the leading order terms  $e_0$  and  $h_0$  are characterized by solutions to quasi-static electromagnetic problems that can be written in terms of electrostatic and magnetostatic resonances.

**Theorem 2.1.** The leading order H field,  $h_0$ , is continuous and divergence free in Y. Moreover, there is a periodic potential w and constant vector  $\mathbf{c}$  such that  $h_0 = \nabla w + \mathbf{c}$  on  $Y \setminus R$  with  $\Delta w = 0$  there. Inside R, the quasi-static magnetic field  $h_0$  solves the Helmholtz equation

$$\nabla \times \nabla \times h_0 = \xi_0 h_0 \quad in \ R, \tag{2.1}$$

where  $\xi_0 = \epsilon_{r,rel} \, \omega_0^2 / c^2$ .

The effective magnetic activity is determined by the volume average of the leading order term  $h_0$ . This is described with the aid of the geometric average  $\oint h_0$  of  $h_0$ . To describe the geometric average consider a smooth vector field v defined on Y/R and periodic on the boundary of Y and introduce

$$\int_{\Gamma_{k,x}} \boldsymbol{v} \cdot \tilde{\mathbf{e}}^k \, \mathrm{d}\ell,$$

with  $\Gamma_{k,x}$  being a curve connecting two points x and  $x + \tilde{\mathbf{e}}^k$  on opposite faces of the unit cube Y and arclength element  $\mathrm{d}\ell$ . Here,  $\Gamma_{k,x}$  can be any such curve lying outside of R. The geometric average  $\oint v$  exists if

$$\left( \oint \mathbf{v} \right) \cdot \tilde{\mathbf{e}}^k := \int_{\varGamma_{k,x}} \mathbf{v} \cdot \tilde{\mathbf{e}}^k \, \mathrm{d}\ell$$

is a unique constant vector independent of the choice of  $\Gamma_{k,x}$ , k = 1, 2, 3. This is always the case when  $\nabla \times \mathbf{v} = 0$  in  $Y \setminus R$  (see [31]). When  $\nabla \times \mathbf{v} = 0$  in Y then  $\oint \mathbf{v} = \int_Y \mathbf{v}$ .

For  $h_0$ , one has the following.

**Corollary 2.2.** The geometric average of  $h_0$  is c, where the constant vector c is defined in theorem 2.1.

The effective magnetic permeability [24,31,32] is defined to be the tensor  $\mu_{\rm eff} = \mu_{\rm eff}(\omega_0)$  relating the volume average to the geometric average of the  $h_0$  field given by

$$\mu_{\text{eff}}\left(\oint h_0\right) = \int_Y h_0(y) \, \mathrm{d}y. \tag{2.2}$$

The explicit formula for  $\mu_{\text{eff}}$  is given in theorem 2.7 and is constructed in §3e.

The  $e_0$  field is the quasi-static electric field inside a periodic composite. We can write  $e_0$  as the sum of a potential gradient  $\nabla \chi$  and a constant vector  $\tilde{\mathbf{e}}$  where  $\chi$  is periodic on Y. We set

$$a_p(y) = \begin{cases} 1 & y \in M \\ \varepsilon_{p,\text{rel}}(\omega_0) & y \in P \end{cases}$$
 (2.3)

and we have the following.

**Theorem 2.3.** The leading order term  $e_0$  satisfies

$$\begin{array}{cccc} \nabla \times e_0 = 0 & in \ Y, \\ e_0 = \nabla \chi + \tilde{e} & in \ Y, \\ e_0 = 0 & in \ R, \end{array}$$
 (2.4)

and

with  $\tilde{\mathbf{e}} = \int_{Y} e_0 \, dy$  and the potential  $\chi$  satisfies

$$\nabla \cdot (a_p(\nabla \chi + \tilde{e})) = 0 \quad \text{in } M \cup P$$

$$n \cdot \varepsilon_{p,\text{rel}}(\omega_0)(\nabla \chi + \tilde{e})\big|_{\partial P^-} = n \cdot (\nabla \chi + \tilde{e})\big|_{\partial P^+},$$
(2.5)

and with

Downloaded from https://royalsocietypublishing.org/ on 16 August 2022

$$\chi + \tilde{e} \cdot x = 0 \quad \text{in R}, \tag{2.6}$$

where  $|_{\partial P^-}$  and  $|_{\partial P^+}$  denote evaluation of quantities on the boundary of P from the inside and outside, respectively, and  $\mathbf{x} = (x_1, x_2, x_3)$  in the space.

We note that  $\chi$  depends linearly on  $\tilde{\mathbf{e}}$  and in the sequel we indicate this by writing  $\chi = \chi^{\tilde{\mathbf{e}}}$ . The effective dielectric constant gives the linear map between an imposed constant electric field and the resulting average dielectric displacement seen by an observer outside the unit period cell and is denoted by  $\epsilon_{\rm eff} = \epsilon_{\rm eff}(\omega_0)$  given by

$$\epsilon_{\text{eff}} \int_{\gamma} e_0 \, \mathrm{d}x = \int_{\partial \gamma} x \boldsymbol{n} \cdot e_0 \, \mathrm{d}s, \tag{2.7}$$

where  $\partial Y$  denotes the boundary of Y and ds is the surface area element. This formula was obtained earlier in the absence of frequency dependent dielectric inclusions in [24,31,32]. The explicit formula for  $\epsilon_{\rm eff}$  as a function of  $\omega_0$  is given in theorem 2.7 and constructed using generalized electrostatic resonances in §3e.

# (b) Homogenized fields

**Theorem 2.4.** (1) The plane waves (homogenized H field)  $H_{hom}(x, t)$  and the homogenized magnetic field  $B_{hom}(x)$  are given by

$$H_{hom}(x,t) = (\oint h_0) e^{(ik\hat{k}\cdot x - i\omega_0 t)}$$

$$B_{hom}(x,t) = \mu_0 \mu_{\text{eff}} H_{hom}(x,t),$$
(2.8)

and

where  $\mu_{\text{eff}}$  is the effective magnetic permeability tensor.

(2) The plane waves (homogenized E field)  $E_{hom}(x,t)$  and the homogenized electric displacement field  $D_{hom}(x)$  are given by

$$E_{hom}(x,t) = \int_{Y} e_0 \, dx \, e^{(ik\hat{k}\cdot x - i\omega_0 t)}$$

$$D_{hom}(x,t) = \epsilon_0 \epsilon_{\text{eff}} E_{hom}(x,t),$$
(2.9)

and

where  $\epsilon_{\it eff}$  is the effective dielectric permittivity tensor.

The homogenized fields are the plane wave solutions of Maxwell's equations for the homogeneous effective media:

$$\nabla \times E_{hom} = -\mu_0 \mu_{\text{eff}} \frac{\partial H_{hom}}{\partial t},$$

$$\nabla \cdot D_{hom} = 0,$$

$$\nabla \times H_{hom} = \epsilon_0 \epsilon_{\text{eff}} \frac{\partial E_{hom}}{\partial t}$$

$$\nabla \cdot H_{hom} = 0.$$
(2.10)

and

Downloaded from https://royalsocietypublishing.org/ on 16 August 2022

The homogenized dispersion relation for the electromagnetic waves travelling through the metamaterial crystal is given by the following theorem.

**Theorem 2.5.** For given  $\hat{k}$  and k, the frequencies  $\omega_0$  for which plane waves can propagate with polarization  $\oint h_0$  in the direction  $\hat{k}$  at wavelength  $\lambda = k/2\pi$  are the roots of the equation

$$\det \left[ k^2 A(\omega_0) + \frac{\omega_0^2}{c^2} \mu_{\text{eff}}(\omega_0^2) \right] = 0, \tag{2.11}$$

with  $\mathbf{A}_{ij}(\omega_0) = \mathcal{E}_{ipm}\hat{k}_p\mathcal{E}_{mnj}[\boldsymbol{\epsilon}_{eff}^{-1}(\omega_0)]_{np}\hat{k}_p$ , i, p, m, n, j = 1, 2, 3 where  $\mathcal{E}_{ipm}$  and  $\mathcal{E}_{mnj}$  are the symbols for the Levi-Civita tensors.

An admissible polarization of the (homogenized H field)  $H_{hom}(x,t)$  field  $\oint \mathbf{h_0}$  lies in the null space of the matrix

$$\[ k^2 A(\omega_0) + \frac{\omega_0^2}{c^2} \mu_{\text{eff}}(\omega_0^2) \] . \tag{2.12}$$

Using equation (2.11), we will find crystal geometries having frequency regimes where  $\mu_{\rm eff}$  and  $\epsilon_{\rm eff}$  are both positive, both negative or band gaps for the metamaterial.

Elimination of  $E_{\text{hom}}$  or  $H_{\text{hom}}$  from (2.10) gives the following.

**Theorem 2.6.** The homogenized fields satisfy the following vector wave equations for a homogeneous effective medium.  $H_{hom}(x, t)$  satisfies

$$\nabla \times \epsilon_{\text{eff}}^{-1} \nabla \times H_{hom}(x, t) = -\frac{1}{c^2} \mu_{\text{eff}} \frac{\partial^2 H_{hom}(x, t)}{\partial t^2}, \tag{2.13}$$

and  $E_{hom}(x,t)$  satisfies

$$\nabla \times \boldsymbol{\mu}_{\mathrm{eff}}^{-1} \nabla \times E_{hom}(\boldsymbol{x}, t) = -\frac{1}{c^2} \epsilon_{\mathrm{eff}} \frac{\partial^2 E_{hom}(\boldsymbol{x}, t)}{\partial t^2}.$$
 (2.14)

# (c) Effective property tensors as functions of frequency

**Theorem 2.7.** (1) The effective magnetic permeability tensor  $\mu_{\text{eff}}$  is given by

$$\boldsymbol{\mu}_{\text{eff}}(\omega_0) = \sum_{n=1}^{\infty} \frac{\omega_0^2/c^2}{\lambda_n \epsilon_{r,\text{rel}}^{-1} - \omega_0^2/c^2} \left( \int_Y \overline{\phi}_n \right) \otimes \left( \int_Y \phi_n \right) + \boldsymbol{I}^3, \tag{2.15}$$

where  $\oint \phi_n = 0$  and  $(\lambda_n, \phi_n)$ ,  $n = 1, 2, \dots$  are the eigenpairs of the following eigenvalue problem:

$$\nabla \times \nabla \times \phi_n = \lambda_n \phi_n \quad \text{in } R,$$

$$\phi_n = \nabla \phi_n \quad \text{in } Y \setminus R$$

$$\Delta \phi_n = 0 \quad \text{in } Y \setminus R$$

$$(2.16)$$

and

with scalar potentials  $\varphi_n$  periodic on Y and on the boundary of R one has continuity of the normal components  $\phi_n \cdot n|^- = \nabla \varphi_n \cdot n|^+$ , where  $|^+$  and  $|^-$  denote limits from the inside and outside of the boundary of R and n is the outward directed unit normal to the boundary.

oyalsocietypublishing.org/journal/rspa Proc. R. Soc. A **478**: 20220194

(2) The effective dielectric permittivity tensor  $\epsilon_{eff}$  is given by

$$\epsilon_{\text{eff}} \tilde{e} \cdot \tilde{e} = (\varepsilon_{p,\text{rel}}(\omega_0)\theta_P + \theta_M)\tilde{e} \cdot \tilde{e}$$

$$+ \theta_{Y \setminus R} \sum_{n=1}^{\infty} (1 + \mu_n(\varepsilon_{p,\text{rel}}(\omega_0) - 1))(a_n + b_n)^2$$

$$+ \int_M \nabla q \cdot \nabla q + \varepsilon_{p,\text{rel}}(\omega_0) \int_P \nabla q \cdot \nabla q, \qquad (2.17)$$

where

$$a_{n} = -\tilde{e} \cdot \frac{\int_{M} \nabla \overline{\psi}_{\mu_{n}} + \varepsilon_{p,\text{rel}}(\omega_{0}) \int_{P} \nabla \overline{\psi}_{\mu_{n}}}{1 - \mu_{n} + \varepsilon_{p,\text{rel}}(\omega_{0}) \mu_{n}}$$
(2.18)

and

$$b_{n} = -\frac{\int_{M} \nabla q \cdot \nabla \overline{\psi}_{\mu_{n}} + \varepsilon_{p,\text{rel}}(\omega_{0}) \int_{P} \nabla q \cdot \nabla \overline{\psi}_{\mu_{n}}}{1 - \mu_{n} + \varepsilon_{p,\text{rel}}(\omega_{0}) \mu_{n}}.$$
(2.19)

Here,  $\theta_P$ ,  $\theta_M$ ,  $\theta_{Y\setminus R}$  are the volumes of P, M and  $Y\setminus R$ , respectively, and  $\psi_{\mu_n}$  are the electrostatic eigenfunctions associated with the eigenvalues  $0 \le \mu_n \le 1$  of the generalized electrostatic resonance eigenvalue problem [17,27]:

$$\Delta \psi_{\mu_{n}} = 0 \quad in \ Y \setminus R,$$

$$\mu_{n} \nabla \psi_{\mu_{n}} \cdot n \big|_{\partial P^{+}} = (\mu_{n} - 1) \nabla \psi_{\mu_{n}} \cdot n \big|_{\partial P^{-}}$$

$$\psi_{\mu_{n}} \big|_{\partial R}^{+} = 0,$$
(2.20)

and

and  $\psi_{\mu_n}$  is continuous in Y \ R, and satisfies periodic boundary conditions on Y. The Y-periodic continuous function q with square integrable derivatives satisfies  $\Delta q = 0$  in  $Y \setminus R$  and  $q = -\tilde{e} \cdot x$  in R.

# Simulation

To frame the discussion, if we assume that the material is isotropic, then for this medium, the dispersion relation is given by

$$\xi_0 = \varepsilon_{r,\text{rel}} k^2 \epsilon_{\text{eff}}^{-1} \ \mu_{\text{eff}}^{-1}, \tag{2.21}$$

where  $\epsilon_{\rm eff}$ ,  $\mu_{\rm eff}$  are constants appearing in the formulae for  $\epsilon_{\rm eff} = \epsilon_{\rm eff} {\bf I}^3$  and  $\mu_{\rm eff} = \mu_{\rm eff} {\bf I}^3$ . Equation (2.21) shows the existence of  $\xi_0$  such that both  $\epsilon_{\rm eff}$  and  $\mu_{\rm eff}$  are negative. As a demonstration, we considered cases where the metamaterial consists of unit cells in which the plasmonic coating and high dielectric core are concentric spheres located at the centre of the cube as shown in figure 2.

In numerical computation of effective magnetic permeability, the following equivalent form of the formula (2.15) is used:

$$\boldsymbol{\mu}_{\mathrm{eff}}(\xi_0) := \mathbf{I}_3 + \frac{1}{4} \sum_{n \in \mathbb{N}} \frac{\xi_0}{1 - \alpha_n \xi_0} \left( \int_R \boldsymbol{y} \times f_n \, \mathrm{d} \boldsymbol{y} \right) \otimes \left( \int_R \boldsymbol{y} \times f_n \, \mathrm{d} \boldsymbol{y} \right), \tag{2.22}$$

where  $(\alpha_n, f_n)$  are the eigenpairs of the following eigenvalue problem:

$$\int_{Y} \nabla \Theta_{f} : \nabla \Theta_{g} \, dx + \frac{1}{4} \left( \int_{R} x \times f \, dx \right) \cdot \left( \int_{R} x \times g \, dx \right) = \alpha \int_{Y} f \cdot g \, dx, \tag{2.23}$$

where g is a vector valued square integrable function such that

$$g = 0$$
 in  $Y \setminus R$  and  $\nabla \cdot g = 0$ .

In equation (2.23), for any function h,  $\Theta_h$  is constructed as follows:

$$-\Delta\Theta_h = h$$
, in  $Y$ ,  $\int_Y \Theta_h = 0$ , (2.24)

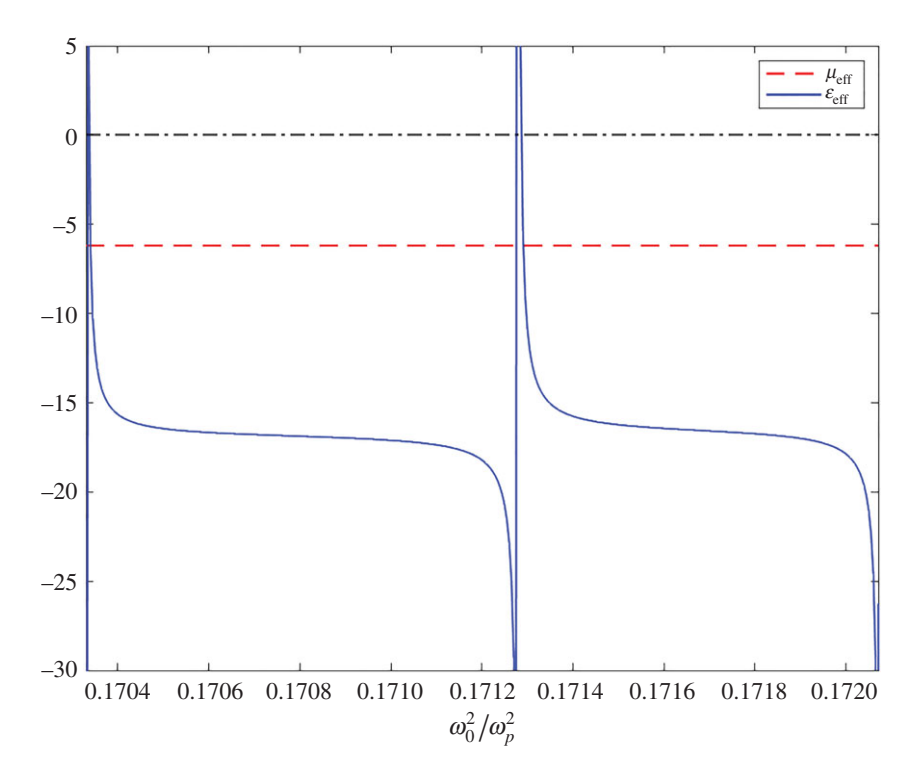


**Figure 3.** The case for R = 0.26, r = 0.156. (Online version in colour.)

where  $\Theta_h$  is periodic. The numerical solutions of both (2.23) and (2.24) are obtained by applying the finite-element method (FEM) via FELICITY [33] in MATLAB. In order to accommodate the divergence free condition for the solution of (2.23), the solution space is discretized using the lowest order Raviart–Thomas finite elements. The solution space for (2.24) is discretized by using first-order Lagrange elements.

In order to compute the effective dielectric tensor formula (2.17), we need to compute both the eigenpairs  $(\psi_{\mu_n}, \mu_n)$  and q. The eigenpairs  $(\psi_{\mu_n}, \mu_n)$  are found by solving (2.20) and the periodic function q is computed by solving the equation

$$\Delta q = 0, \quad q \big|_{\partial R^+} = -\tilde{e} \cdot x.$$
 (2.25)

Both problems (2.20) and (2.25) are solved via FELICITY [33] in MATLAB by applying FEM. The solution spaces are discretized by using first-order Lagrange elements.

For the inclusions, we chose dielectric constant  $\varepsilon_{r,\mathrm{rel}}=1$  and  $\xi_p=3\times 10^{15}$  for the plasmon frequency of the plasmonic coating which was assumed to be made of gold. We considered five different cases where the geometry is given by different radii for the concentric spherical inclusions. In the first three cases, we identified two intervals for  $\xi_0/\xi_p=\omega_0^2/\omega_p^2$ , where  $\epsilon_{\mathrm{eff}}$  and  $\mu_{\mathrm{eff}}$  are negative. This corresponds to the wave propagating in the direction opposite to the wave velocity. This is seen in [23] for transverse magnetic transmission.

The first three cases, shown in figures 3–5, demonstrate the intervals where both effective magnetic permeability and effective dielectric permittivity exhibit negative behaviour. In these graphs, *R* and *r* denote the radii of the plasmonic and high dielectric inclusions, respectively.

To illustrate other behaviours of effective properties, we identified two frequency intervals, shown in figure 6, where we observe that the effective magnetic permeability is positive while the effective dielectric permittivity remains negative. These intervals correspond to band gaps. Figure 7 illustrates the case of a frequency interval where both effective properties exhibit positive behaviour and waves propagate along the direction of the phase velocity. In this case,

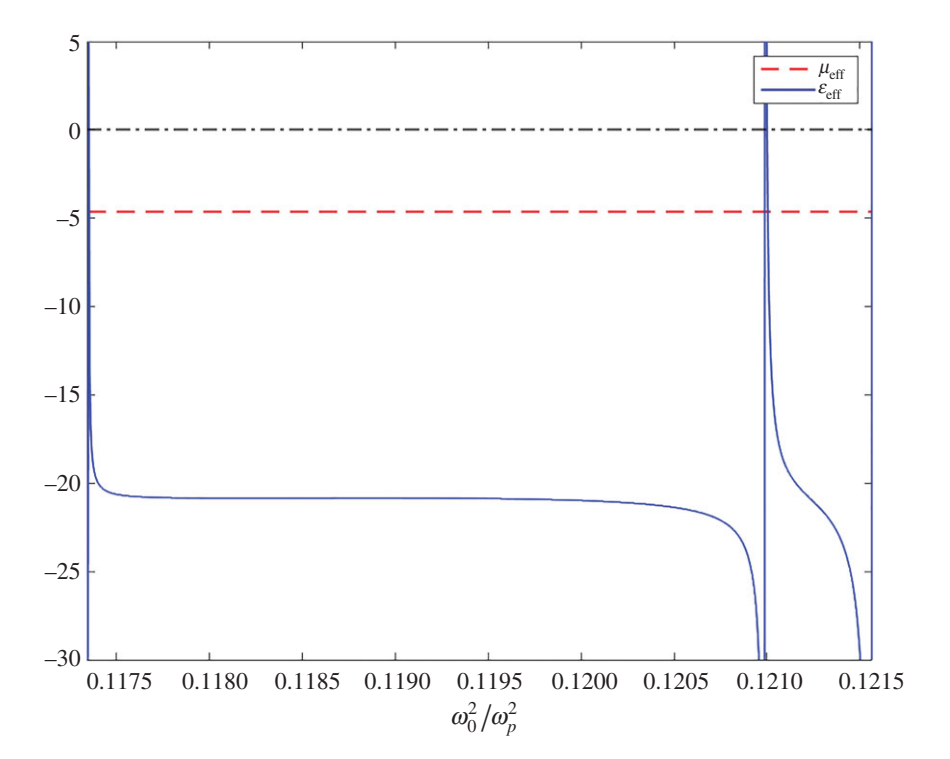


**Figure 4.** The case for R = 0.3, r = 0.12. (Online version in colour.)

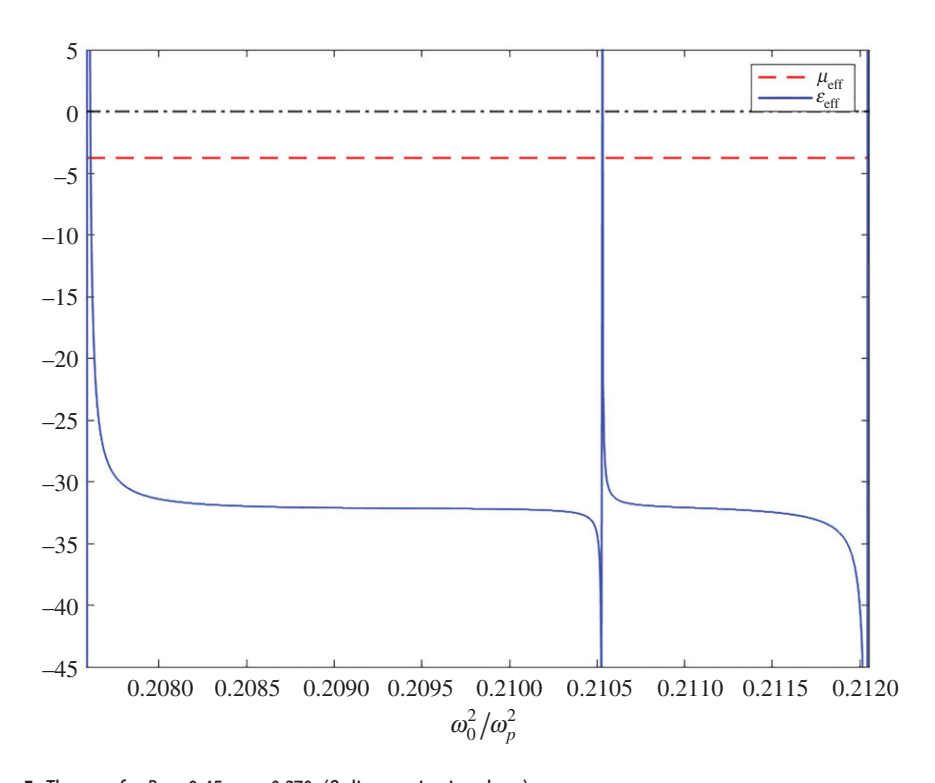


**Figure 5.** The case for R = 0.45, r = 0.270. (Online version in colour.)

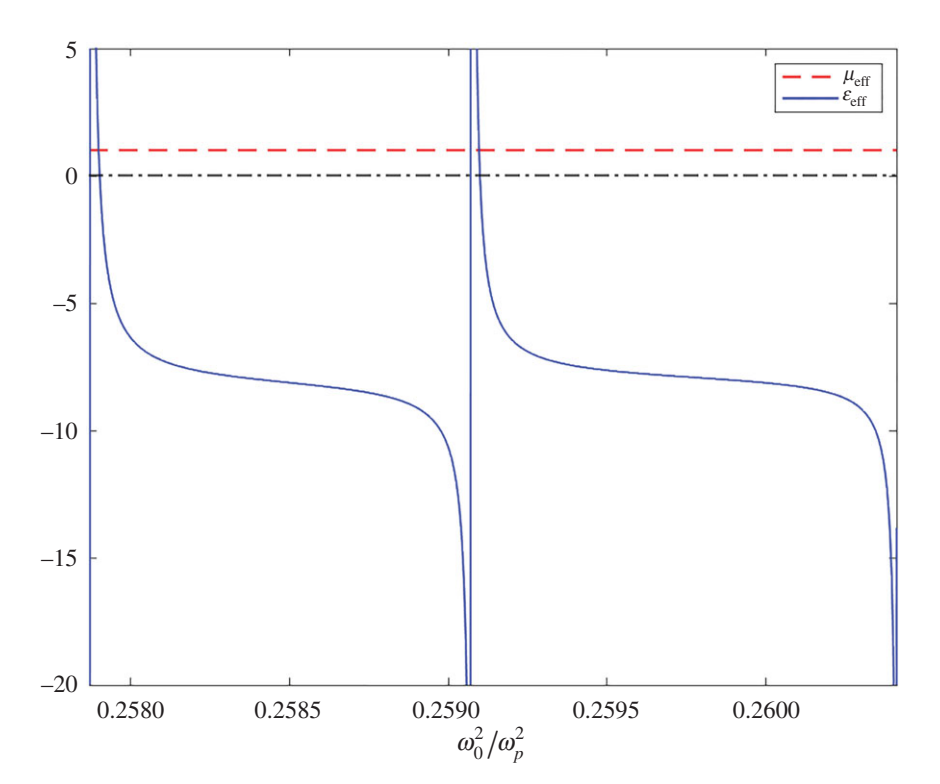


**Figure 6.** The case for R = 0.35, r = 0.14. (Online version in colour.)

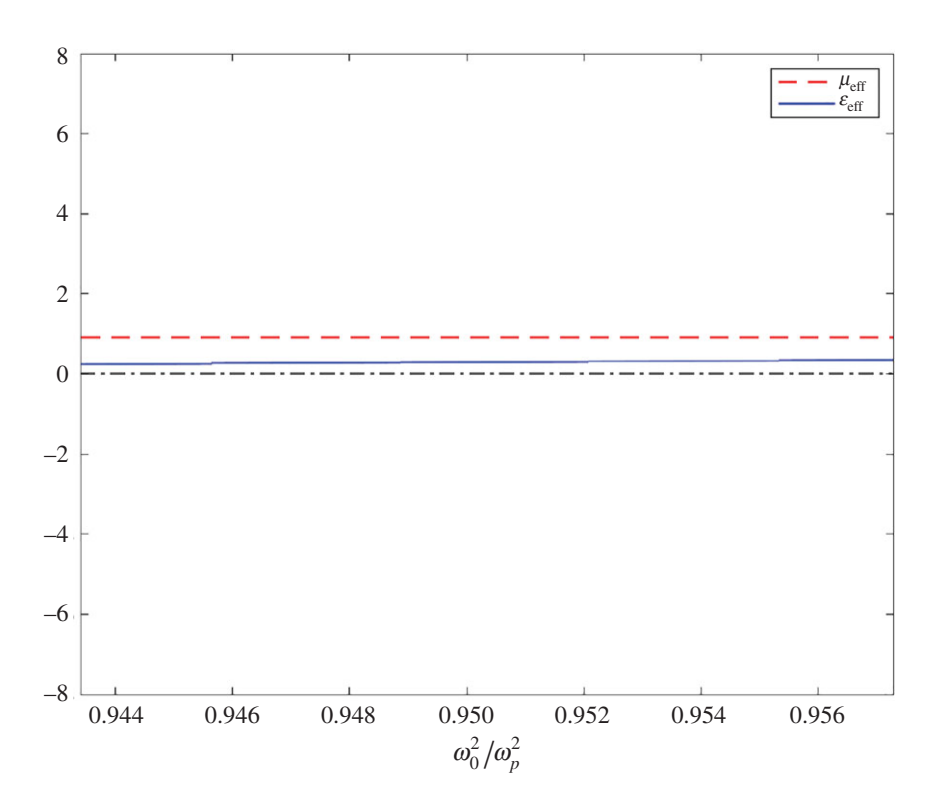


**Figure 7.** The case for R = 0.45, r = 0.18. (Online version in colour.)

we observe that the effective dielectric permittivity exhibits positive behaviour when  $\xi_0$  is close to the plasmon frequency of the gold.

By writing the formula (2.22) as

$$\boldsymbol{\mu}_{\text{eff}}\left(\frac{\omega_0^2}{\omega_p^2}\right) = \mathbf{I}_3 + \frac{1}{4} \sum_{n \in \mathbb{N}} \frac{\omega_0^2/\omega_p^2}{(1/\xi_p) - \alpha_n(\omega_0^2/\omega_p^2)} \left(\int_R \boldsymbol{y} \times f_n \, \mathrm{d}\boldsymbol{y}\right) \otimes \left(\int_R \boldsymbol{y} \times f_n \, \mathrm{d}\boldsymbol{y}\right), \tag{2.26}$$

it can be seen that, except for the poles of effective permeability tensor that are very close to 0, the graph of effective permeability is a horizontal line in all of the cases considered.

Figure 3 illustrates the case where the plasmonic inclusion has radius R = 0.26 and the high dielectric inclusion has radius r = 0.156. For this case, we identify two frequency intervals [0.17033, 0.171277] and [0.17128, 0.17207] where both effective tensors are negative. Figure 4 illustrates the case where the plasmonic inclusion has radius R = 0.3 and the high dielectric inclusion has radius r = 0.12. Here, we have identified two frequency intervals [0.117425, 0.120897] and [0.121006, 0.1215221] where both effective tensors are negative. Figure 5 illustrates the case where the plasmonic inclusion has radius R = 0.45 and the high dielectric inclusion has radius r = 0.27. For this case, we identify two frequency intervals [0.207610, 0.2105] and [0.210773, 0.21203] where both effective tensors are negative. Figure 6 illustrates the case where the plasmonic inclusion has radius R = 0.35 and the high dielectric inclusion has radius r =0.14. For this case, we identify two frequency intervals [0.25797, 0.259008] and [0.25910, 0.26041] where the effective magnetic permeability is positive while the effective dielectric permittivity is negative. Figure 7 illustrates the case where the plasmonic inclusion has radius R = 0.45and the high dielectric inclusion has radius r = 0.18. For this case, we identify a frequency interval [0.94342, 0.95728] where both the effective magnetic permeability tensor and the effective dielectric tensor are positive.

### 3. Proof of results

# Leading order terms in power series and metamaterial

We carry out the analysis for the configuration shown in figure 1, noting that a nearly identical analysis can be carried out for the coated sphere geometry with the obvious modifications. To expedite the asymptotic analysis, we introduce the non-dimensional square frequency  $\xi =$  $(\varepsilon_{r,\text{rel}}\omega^2)/c^2$ , square plasma frequency  $\xi_p = (\omega_p^2 \varepsilon_{r,\text{rel}})/c^2$  and period size  $\rho = d/\sqrt{\varepsilon_{r,\text{rel}}}$ , where  $\omega_p$ is the plasmon frequency of the inclusion P. The non-dimensional wavenumber is written  $\tau =$  $\sqrt{k^2 \varepsilon_{r,\text{rel}}}$ .

We now recover the homogenization theorems. Substitution of

$$\begin{split} \mathcal{E}(y) &= e_0(y) \, \mathrm{e}^{\mathrm{i} \eta \hat{k} \cdot y} + e_1(y) \eta \, \mathrm{e}^{\mathrm{i} \eta \hat{k} \cdot y} + e_2(y) \eta^2 \, \mathrm{e}^{\mathrm{i} \eta \hat{k} \cdot y} + \cdots \, , \\ \mathcal{H}(y) &= h_0(y) \, \mathrm{e}^{\mathrm{i} \eta \hat{k} \cdot y} + h_1(y) \eta \, \mathrm{e}^{\mathrm{i} \eta \hat{k} \cdot y} + h_2(y) \eta^2 \, \mathrm{e}^{\mathrm{i} \eta \hat{k} \cdot y} + \cdots \\ \sqrt{\xi} &= \sqrt{\xi_0} + \sqrt{\xi_1} \eta + \sqrt{\xi_2} \eta^2 + \cdots \end{split}$$

and

into (1.4) gives the following.

— In R

$$\tau[(\nabla \times e_0 + i\eta \hat{k} \times e_0) + \eta(\nabla \times e_1 + i\eta \hat{k} \times e_1) + \cdots]$$

$$= i\eta n_0(\sqrt{\xi_0} + \sqrt{\xi_1}\eta + \cdots)(h_0 + \eta h_1 + \cdots), \tag{3.1}$$

$$\eta[(\nabla \times h_0 + i\eta \hat{k} \times h_0) + \eta(\nabla \times h_1 + i\eta \hat{k} \times h_1) + \cdots] 
= -i\tau n_0^{-1} (\sqrt{\xi_0} + \sqrt{\xi_1}\eta + \cdots) (e_0 + \eta e_1 + \cdots).$$
(3.2)

— In P

$$\tau[(\nabla \times e_0 + i\eta \hat{k} \times e_0) + \eta(\nabla \times e_1 + i\eta \hat{k} \times e_1) + \cdots]$$

$$= i\eta n_0(\sqrt{\xi_0} + \sqrt{\xi_1}\eta + \cdots)(h_0 + \eta h_1 + \cdots), \tag{3.3}$$

$$\tau[(\nabla \times h_0 + i\eta \hat{k} \times h_0) + \eta(\nabla \times h_1 + i\eta \hat{k} \times h_1) + \cdots]$$
  
=  $-i\eta n_0^{-1} (\sqrt{\xi_0} + \eta \sqrt{\xi_1} + \cdots) (1 - \xi^*) (e_0 + \eta e_1 + \cdots),$  (3.4)

where

$$\xi^* = \frac{\xi_p}{(\sqrt{\xi_0} + \eta \sqrt{\xi_1} + \cdots)^2}.$$

— In M

$$\tau[(\nabla \times e_0 + i\eta \hat{k} \times e_0) + \eta(\nabla \times e_1 + i\eta \hat{k} \times e_1) + \cdots]$$

$$= i\eta n_0(\sqrt{\xi_0} + \sqrt{\xi_1}\eta + \cdots)(h_0 + \eta h_1 + \cdots), \tag{3.5}$$

$$\tau[(\nabla \times h_0 + i\eta \hat{k} \times h_0) + \eta(\nabla \times h_1 + i\eta \hat{k} \times h_1) + \cdots]$$

$$= -i\eta n_0^{-1} (\sqrt{\xi_0} + \sqrt{\xi_1}\eta + \cdots) (e_0 + \eta e_1 + \cdots). \tag{3.6}$$

On R-M interface

$$n \cdot (e_0 + \eta e_1 + \cdots)|_{\partial R^-} = \rho^2 n \cdot (e_0 + \eta e_1 + \cdots)|_{\partial R^+},$$
 (3.7)

$$n \times (e_0 + \eta e_1 + \cdots)|_{\partial R^-} = n \times (e_0 + \eta e_1 + \cdots)|_{\partial R^+}.$$
 (3.8)

On P–M interface

$$n \cdot \left[ \left( \sqrt{\xi_0} + \eta \sqrt{\xi_1} + \cdots \right)^2 - \xi_r \right] (e_0 + \eta e_1 + \cdots) \big|_{\partial P^-}$$

$$= n \cdot \left( \sqrt{\xi_0} + \eta \sqrt{\xi_1} + \cdots \right)^2 (e_0 + \eta e_1 + \cdots) \big|_{\partial P^+}$$
(3.9)

$$n \times (e_0 + \eta e_1 + \cdots)|_{\partial P^-} = n \times (e_0 + \eta e_1 + \cdots)|_{\partial P^+}.$$
 (3.10)

We also have

Downloaded from https://royalsocietypublishing.org/ on 16 August 2022

— In R

$$(\nabla \cdot e_0 + i\eta \hat{k} \cdot e_0) + \eta (\nabla \cdot e_1 + i\eta \hat{k} \cdot e_1) + \dots = 0.$$
 (3.11)

— In Р

$$\varepsilon_{p,\text{rel}}[(\nabla \cdot e_0 + i\eta \hat{k} \cdot e_0) + \eta(\nabla \cdot e_1 + i\eta \hat{k} \cdot e_1) + \cdots] = 0.$$
(3.12)

— In M

$$(\nabla \cdot e_0 + i\eta \hat{k} \cdot e_0) + \eta(\nabla \cdot e_1 + i\eta \hat{k} \cdot e_1) + \dots = 0.$$
(3.13)

On R–M interface

$$n \cdot \frac{1}{\rho^2} e_i \big|_{\partial R^-} = n \cdot e_i \big|_{\partial R^+}. \tag{3.14}$$

— On P–M interface

$$n \cdot \varepsilon_{p,\text{rel}} e_i \big|_{\partial P^-} = n \cdot e_i \big|_{\partial P^+}. \tag{3.15}$$

We now collect like order terms with the same powers of  $\eta$ . We first recover theorem 2.3 by collecting zeroth-order terms in (3.1), (3.3) and (3.5), to get

$$\tau(\nabla \times e_0) = 0 \text{ in R,}$$

$$\tau(\nabla \times e_0) = 0 \text{ in P}$$

$$\tau(\nabla \times e_0) = 0 \text{ in M.}$$
(3.16)

and

From (3.8), (3.10) and (3.15), we have

$$n \times e_{0}|_{\partial R^{-}} = n \times e_{0}|_{\partial R^{+}},$$

$$n \times e_{0}|_{\partial P^{-}} = n \times e_{0}|_{\partial P^{+}}$$

$$\varepsilon_{p,rel}(\omega_{0})n \cdot e_{0}|_{\partial P^{-}} = n \cdot e_{0}|_{\partial P^{+}}.$$
(3.17)

and

From (3.11) to (3.14), we have

$$\nabla \cdot \varepsilon_{p,\text{rel}} e_0 = 0 \quad \text{in P,}$$

$$\nabla \cdot e_0 = 0 \quad \text{in M,}$$

$$\nabla \cdot e_0 = 0 \quad \text{in R}$$

$$n \cdot e_0 \Big|_{\partial R^-} = 0.$$
(3.18)

and

Using (3.16), we find

$$\int_{V} |\nabla \times e_{\mathbf{0}}|^{2} \, \mathrm{d}y = 0. \tag{3.19}$$

So  $\nabla \times e_0 = 0$  in Y and  $e_0$  can be written as

$$e_0 = \nabla \chi^{\tilde{\mathbf{e}}} + \tilde{\mathbf{e}} \quad \text{in } \Upsilon, \tag{3.20}$$

where  $\chi^{\tilde{\mathbf{e}}}$  is a *Y*-periodic potential with square integrable gradient and  $\tilde{\mathbf{e}}$  is a complex vector. Since  $\int_{Y} \nabla \chi^{\tilde{\mathbf{e}}} = 0$ , we get that  $\int_{Y} e_0 = \tilde{\mathbf{e}}$ . Using (3.18) and (3.20), we observe that

$$\int_{\mathbb{R}} |e_0|^2 \, \mathrm{d}y = 0, \tag{3.21}$$

and this implies that  $e_0 = 0$  in R and we have established theorem 2.3.

We show that the transmission problem given by (2.5) and (2.6) follows from the asymptotic expansions. From  $e_0 = \nabla \chi^{\tilde{\mathbf{e}}} + \tilde{\mathbf{e}} = 0$  in R, we discover that  $\chi^{\tilde{\mathbf{e}}} + \tilde{\mathbf{e}} \cdot x = c_0$  in R, where  $c_0$  is a constant scalar. We are free to choose the constant  $c_0 = 0$  and from continuity of the potential across the boundary of R we get

$$\left(\chi^{\tilde{\mathbf{e}}} + \tilde{\mathbf{e}} \cdot \mathbf{x}\right)\big|_{\partial \mathbb{R}^+} = 0,\tag{3.22}$$

and (2.6) follows. The transmission problem given by (2.5) and (2.6) now follows on setting  $e_0 = \nabla \chi^{\tilde{\mathbf{e}}} + \tilde{\mathbf{e}}$  and applying the last equation in (3.17) together with the first two equations in (3.18). From linearity  $\chi^{\tilde{\mathbf{e}}}$  depends linearly on  $\tilde{\mathbf{e}}$  and we can write  $\tilde{\mathbf{e}} = \sum_{k=1}^{3} e_k \tilde{\mathbf{e}}^k$ , for scalars  $e_k$  and

$$\chi^{\tilde{\mathbf{e}}} = \sum_{k=1}^{3} e_k \phi^k, \quad k = 1, 2, 3,$$
 (3.23)

where the potentials  $\phi^k$ , k = 1, 2, 3 solve

$$\nabla \cdot [a_{p}(\mathbf{y})(\nabla \phi^{k} + \tilde{\mathbf{e}}^{k})] = 0 \quad \text{in } M \cup P$$

$$n \cdot \varepsilon_{p,\text{rel}}(\omega_{0})(\nabla \phi^{k} + \tilde{\mathbf{e}}^{k})\big|_{\partial P^{-}} = n \cdot (\nabla \phi^{k} + \tilde{\mathbf{e}}^{k})\big|_{\partial P^{+}}$$
(3.24)

and

$$\phi^k + x_k|_{\partial P^+} = 0. ag{3.25}$$

Given  $\tilde{\mathbf{v}} = \sum_{k=1}^{3} v_k \tilde{\mathbf{e}}^k$  set  $\mathbf{v_0} = \nabla \chi^{\tilde{\mathbf{v}}} + \tilde{\mathbf{v}}$ , where  $\chi^{\tilde{\mathbf{v}}} = \sum_{k=1}^{3} v_k \phi^k$ . The effective bilinear form describing the effective property is defined by

$$\epsilon_{\text{eff}}\tilde{\mathbf{e}}\cdot\tilde{\mathbf{v}} = \int_{Y} \varepsilon_{\text{rel}}^{d}(\nabla\chi^{\tilde{\mathbf{e}}} + \tilde{\mathbf{e}})\cdot(\nabla\chi^{\tilde{\mathbf{v}}} + \tilde{\mathbf{v}})\,\mathrm{d}y. \tag{3.26}$$

An integration by parts of (3.26) recovers the equivalent formulation of the effective dielectric constant given in (2.7).

Now, we recover theorem 2.1. Collecting the zeroth-order terms of  $\eta$  from (3.1) to (3.15), we have

$$\nabla \times h_0 = 0 \quad \text{in } P,$$

$$\nabla \times h_0 = 0 \quad \text{in } M,$$

$$\nabla \cdot h_0 = 0 \quad \text{in } Y$$

$$[h_0] = 0 \quad \text{on } \partial P \text{ and } \partial R.$$

$$(3.27)$$

and

Downloaded from https://royalsocietypublishing.org/ on 16 August 2022

Finally, we write (3.2) as

$$(\nabla + i\eta \hat{k}) \times (h_0 + \eta h_1 + \cdots) = -i \frac{n_0^{-1}}{\rho} \left( \sqrt{\xi_0} + \eta \sqrt{\xi_1} + \cdots \right) (e_0 + \eta e_1 + \cdots). \tag{3.28}$$

By applying the differential operator  $(\nabla + i\eta \hat{k}) \times$  to both sides of (3.28) and collecting the zeroth-order and first-order terms of  $\eta$ , we find that

$$\nabla \times \nabla \times h_0 = \xi_0 h_0 \quad \text{in } R. \tag{3.29}$$

Since  $h_0$  is divergence free on Y and  $\nabla \times h_0 = 0$  on  $Y \setminus R$ , there is a potential w and a constant vector  $\mathbf{c}$  such that  $h_0 = \nabla w + \mathbf{c}$  on  $Y \setminus R$  with  $\Delta w = 0$  there and periodic on the boundary of Y. Theorem 2.1 now follows.

To see theorem 2.2 note that since  $h_0 = \nabla w + \mathbf{c}$ , where w is periodic on the boundary of Y, then direct calculation shows  $\oint h_0 = \mathbf{c}$  for any choice of  $\Gamma_k$ , k = 1, 2, 3.

# (b) Derivation of homogenized fields

We focus now on recovering the homogenized equations (2.10) from the expansions. We collect terms of the first order in  $\eta$  in (3.1), (3.3) and (3.5), and get

$$\tau(\nabla \times e_1) = i\sqrt{\xi_0}n_0h_0 \quad \text{in R,}$$

$$\tau(\nabla \times e_1 + i\hat{k} \times e_0) = i\sqrt{\xi_0}n_0h_0 \quad \text{in P}$$

$$\tau(\nabla \times e_1 + i\hat{k} \times e_0) = i\sqrt{\xi_0}n_0h_0 \quad \text{in M.}$$
(3.30)

and

We integrate the equations in (3.30) over the regions R, P and M, respectively. The summation of these three integrals gives

$$\tau \int_{\gamma} i\hat{k} \times e_0 \, \mathrm{d}y = i n_0 \sqrt{\xi_0} \int_{\gamma} h_0 \, \mathrm{d}y. \tag{3.31}$$

Collecting terms of second order in  $\eta$  in (3.2) and first order in  $\eta$  in (3.4) and (3.6) gives

$$\nabla \times h_{1} + i\hat{k} \times h_{0} = -i\tau n_{0}^{-1} (\sqrt{\xi_{1}} e_{1} + \sqrt{\xi_{0}} e_{2}) \quad \text{in R,}$$

$$\tau (\nabla \times h_{1} + i\hat{k} \times h_{0}) = -i\varepsilon_{p,\text{rel}}(\xi_{0})\sqrt{\xi_{0}} n_{0}^{-1} e_{0} \quad \text{in P}$$

$$\tau (\nabla \times h_{1} + i\hat{k} \times h_{0}) = -i\sqrt{\xi_{0}} n_{0}^{-1} e_{0} \quad \text{in M.}$$
(3.32)

and

On setting  $e^{*,i} = \nabla \phi^i + \tilde{e}^i$ , i = 1, 2, 3, we have

$$e^{*,i} = 0 \text{ in R}, \quad \nabla \cdot e^{*,i} = 0 \text{ in Y} \quad \text{and } \int_{Y} e^{*,i} = \tilde{e}^{i}, \ i = 1, 2, 3.$$
 (3.33)

We multiply equations in (3.32) by  $e^{*,i}$  and then integrate them over the regions R, P and M, respectively. Adding the integrals together gives

$$\tau \left( \int_{Y} \nabla \times h_{1} \cdot \mathbf{e}^{*,i} \, \mathrm{d}y + \int_{Y} i\hat{k} \times h_{0} \cdot \mathbf{e}^{*,i} \, \mathrm{d}y \right) = -in_{0}^{-1} \sqrt{\xi_{0}} \int_{Y} \varepsilon_{\mathrm{rel}}^{d}(\xi_{0}, y) e_{0} \cdot \mathbf{e}^{*,i} \, \mathrm{d}y. \tag{3.34}$$

Applying the definition of the effective magnetic permeability (2.2) to the equation (3.31), we obtain

$$\tau \hat{k} \times \left( \int_{Y} e_{0} \right) = n_{0} \sqrt{\xi_{0}} \mu_{\text{eff}} \left( \oint h_{0} \right). \tag{3.35}$$

Note that  $\nabla \times e_0 = 0$  in Y implies  $\nabla \times e^{*,i} = 0$  in Y. So we can show  $\nabla \cdot (e^{*,i} \times k) = 0$ . Therefore, an application of lemma 4.5 of [24] to the second term of the left-hand side of (3.34) gives

$$i\tau \int_{Y} \hat{k} \times h_{0} \cdot \mathbf{e}^{*,i} \, \mathrm{d}y = i\tau \int_{Y} h_{0} \cdot (\hat{k} \times \mathbf{e}^{*,i})$$
$$= i\tau (\hat{k} \times \phi h_{0}) \cdot \tilde{\mathbf{e}}^{i}. \tag{3.36}$$

A direct calculation gives

$$\int_{\Upsilon} \nabla \times \mathbf{h}_1 \cdot \mathbf{e}^{*,i} = 0. \tag{3.37}$$

Finally, applying (3.37) and (3.36) in (3.34) gives

$$i\tau(\hat{k}\times\oint h_0)\cdot\tilde{\mathbf{e}}^i = -in_0^{-1}\sqrt{\xi_0}\int_{Y}\varepsilon_{\mathrm{rel}}^d(\xi_0,y)(\nabla\chi^{\tilde{\mathbf{e}}}+\tilde{\mathbf{e}})\cdot\mathbf{e}^{*,i}\,\mathrm{d}y. \tag{3.38}$$

From linearity, we express the effective dielectric permittivity tensor  $\epsilon_{
m eff}$  as

$$[\boldsymbol{\epsilon}_{\text{eff}}]_{ij} := \int_{Y} \varepsilon_{\text{rel}}^{d}(\xi_{0}, \boldsymbol{y}) \mathbf{e}^{*,i} \cdot \mathbf{e}^{*,j} \, \mathrm{d}\boldsymbol{y}, \tag{3.39}$$

and (3.38) and (3.39) give

Downloaded from https://royalsocietypublishing.org/ on 16 August 2022

$$\int_{Y} e_{\mathbf{0}} \, \mathrm{d}y = -\tau \, \frac{n_{\mathbf{0}}}{\sqrt{\xi_{\mathbf{0}}}} \epsilon_{\mathrm{eff}}^{-1} (\hat{k} \times \oint h_{\mathbf{0}}). \tag{3.40}$$

Substituting (3.40) into (3.35) gives

$$-\tau^2 \hat{k} \times \epsilon_{\text{eff}}^{-1} \hat{k} \times \oint h_0 = \xi_0 \mu_{\text{eff}} \oint h_0, \tag{3.41}$$

which then yields

$$\nabla_{x} \times \epsilon_{\text{eff}}^{-1} \nabla_{x} \times \oint h_{0} e^{ik\hat{k} \cdot x} = \frac{\omega_{0}^{2}}{c^{2}} \mu_{\text{eff}} \oint h_{0} e^{ik\hat{k} \cdot x}.$$
 (3.42)

Multiplying by  $e^{-i\omega_0 t}$  both sides of (3.42) and noting that  $H_{\text{hom}}(x,t) = \left(\oint h_0\right) e^{(i\hat{k}\hat{k}\cdot x - i\omega_0 t)}$  completes the proof of (2.13).

By expressing  $\oint h_0$  in (3.35) and using (3.38), we get

$$\nabla_{x} \times \boldsymbol{\mu}_{\mathrm{eff}}^{-1} \times \int_{Y} e_{0} \, \mathrm{e}^{\mathrm{i}k\hat{k}\cdot x} = \frac{\omega_{0}^{2}}{c^{2}} \boldsymbol{\varepsilon}_{\mathrm{eff}} \int_{Y} e_{0} \, \mathrm{e}^{\mathrm{i}k\hat{k}\cdot x}.$$

Multiplying by  $e^{-i\omega_0 t}$  both sides and noting that  $E_{\text{hom}}(x,t) = \int_Y e_0 \, dx \, e^{(ik\hat{k}\cdot x - i\omega_0 t)}$  completes the proof of (2.14).

# (c) Derivation of Maxwell's system for homogenized fields

Using equations (3.35), (3.40), and  $n_0 = \sqrt{\mu_0/\varepsilon_0}$ ,  $c = 1/\sqrt{\mu_0\varepsilon_0^2}$ ,  $\sqrt{\xi_0} = (\omega_0/c)\sqrt{\varepsilon_{r,\text{rel}}}$ , we find

$$\nabla_{x} \times \left( \int_{Y} e_{0} e^{ik\hat{k} \cdot x} \right) = i\varepsilon_{0}\omega_{0} \mu_{\text{eff}}(\oint h_{0} e^{ik\hat{k} \cdot x})$$

and

$$\nabla_{x} \times (\oint_{Y} h_{0} e^{ik\hat{k}\cdot x}) = -i\mu_{0}\omega_{0} \varepsilon_{\text{eff}} \left( \int e_{0} e^{ik\hat{k}\cdot x} \right).$$

Finally, multiplying by  $e^{-i\omega_0 t}$  both sides of the above equations and using (2.8) and (2.9) complete the proof of the first and the third equations in (2.10). The second and the fourth equations of (2.10) are the direct consequence of applying the divergence operator to  $H_{hom}$  and  $E_{hom}$  in (2.8) and (2.9).

#### (d) Demonstration of dispersion relation

Using Einstein summation notation and Levi-Civita tensor notations, we have

$$\xi_0 \mu_{\text{eff}}(\xi_0) \oint h_0 = \xi_0 [\mu_{\text{eff}}(\xi_0)]_{ij} \left[ \oint h_0 \right]_i$$
 (3.43)

and

Downloaded from https://royalsocietypublishing.org/ on 16 August 2022

$$\left(\hat{k} \times \left[\boldsymbol{\varepsilon}_{\text{eff}}^{-1}(\xi_0)\hat{k} \times \oint \boldsymbol{h}_0\right]\right)_i = \mathcal{E}_{ipm}\hat{k}_p \mathcal{E}_{mnj}\left[\boldsymbol{\varepsilon}_{\text{eff}}^{-1}(\xi_0)\right]_{np} \hat{k}_p \left[\oint \boldsymbol{h}_0\right]_i, \tag{3.44}$$

where i, p, m, n, j = 1, 2, 3. So equation (3.41) is written by components as

$$0 = \tau^{2} \hat{k} \times \boldsymbol{\varepsilon}_{\text{eff}}^{-1}(\xi_{0}) \hat{k} \times \oint \boldsymbol{h}_{0} + \xi_{0} \boldsymbol{\mu}_{\text{eff}}(\xi_{0}) \oint \boldsymbol{h}_{0}$$

$$= \tau^{2} \mathcal{E}_{ipm} \hat{k}_{p} \mathcal{E}_{mnj} \left[ \boldsymbol{\varepsilon}_{\text{eff}}^{-1}(\xi_{0}) \right]_{np} \hat{k}_{p} \left[ \oint \boldsymbol{h}_{0} \right]_{j} + \xi_{0} \left[ \boldsymbol{\mu}_{\text{eff}}(\xi_{0}) \right]_{ij} \left[ \oint \boldsymbol{h}_{0} \right]_{j}. \tag{3.45}$$

Equation (3.45) implies that the determinant equation for  $\xi_0$  at a given wavenumber k can be written as

 $\begin{aligned}
\det[\tau^{2}\mathbf{A} + \xi_{0}\boldsymbol{\mu}_{\text{eff}}(\xi_{0})] &= 0 \\
\mathbf{A}_{ij} &= \mathcal{E}_{ipm}\hat{k}_{p}\mathcal{E}_{mnj}\left[\boldsymbol{\varepsilon}_{\text{eff}}^{-1}(\xi_{0})\right]_{np}\hat{k}_{p},
\end{aligned} (3.46)$ 

and

where i, p, m, n, j = 1, 2, 3. Noting that  $\tau^2 = k^2 \varepsilon_{r, \text{rel}}, \xi_0 = (\omega_0^2/c^2)\varepsilon_{r, \text{rel}}$  completes the proof.

# (e) Effective property tensors and their meaning as explicit functions of $\xi_0$

The effective permittivity (2.2) and its formula (2.15) follows from an eigenfunction expansion of  $h_0$ . Here, we use the eignfunctions given in theorem 2.7. These eigenfunctions form an complete orthonormal system with respect to the inner product  $(h, w) := \int_Y h \cdot \overline{w} \, dy$ , i.e.  $(\phi_i, \phi_j) = \delta_{ij}$ . It is easily seen as in [24] that  $h_0 - \oint h_0$  lies in the span of  $\{\phi_n\}$  and we write  $h_0 = \sum_{j=1}^\infty c_j \phi_j + \mathbf{c}$ , where  $\mathbf{c} = \oint h_0$  and determine the coefficients  $c_j$ . Substitution into (2.1) gives

$$c_j = \frac{\xi_0 \mathbf{c} \cdot \int_Y \overline{\phi}_j}{\lambda_i - \xi_0}.$$
 (3.47)

So

$$h_0 = \sum_{i=1}^{\infty} \frac{\xi_0 \mathbf{c} \cdot \int_Y \overline{\phi}_j \, \mathrm{d}x}{\lambda_i - \xi_0} \phi_j + \mathbf{c}. \tag{3.48}$$

royalsocietypublishing.org/journal/rspa Proc. R. Soc. A **478**: 2022019

 $\int_{V} h_0 \, \mathrm{d}x = \sum_{i=1}^{\infty} \frac{\xi_0 \, \mathbf{c} \cdot \int_{Y} \overline{\phi}_i \, \mathrm{d}x}{\lambda_i - \xi_0} \int_{Y} \phi_i \, \mathrm{d}x + \mathbf{c}$ (3.49)

$$= \left(\sum_{i=1}^{\infty} \frac{\xi_0}{\lambda_i - \xi_0} \int_{Y} \overline{\phi}_j \, \mathrm{d}x \otimes \int_{Y} \phi_j \, \mathrm{d}x + I\right) \oint h_0 \tag{3.50}$$

$$=\tilde{\boldsymbol{\mu}}_{\mathrm{eff}}(\xi_0) \oint \boldsymbol{h}_0,\tag{3.51}$$

and the formula for  $\mu_{\text{eff}}(\omega_0)$  follows noting that  $\mu_{\text{eff}}(\omega_0) = \tilde{\mu}_{\text{eff}}(\xi_0)$ .

Formula (2.17) follows from an eigenfunction expansion of  $\chi^{\tilde{\mathbf{e}}}$ . Here, we use the eignfunctions given by (2.20). The set of these functions form a complete orthonormal set over the space of continuous functions periodic in Y with zero average and square integrable gradient that are zero in R, with inner product  $\langle \psi, \phi \rangle = \int_{Y/R} \nabla \psi \cdot \nabla \overline{\phi} \, dx$ .

Let

Hence

$$\chi^{\tilde{\mathbf{e}}} = w + r + q,\tag{3.52}$$

where w satisfies

$$\nabla \cdot \left( \varepsilon_{\text{rel}}^{d}(\omega_{0})(\nabla w + \tilde{\mathbf{e}}) \right) = 0 \quad \text{in } Y \setminus R;$$
(3.53)

r satisfies

$$\nabla \cdot \left( \varepsilon_{\text{rel}}^d(\omega_0)(\nabla r + \nabla q) \right) = 0 \quad \text{in } Y \setminus R;$$
(3.54)

and q satisfies  $\Delta q = 0$  in  $Y \setminus R$  and  $q = -\tilde{\mathbf{e}} \cdot x$  in R. The functions w and r admit the eigenfunction expansion

$$w = \sum_{n=1}^{\infty} a_n \psi_{\mu_n}$$
 and  $r = \sum_{n=1}^{\infty} b_n \psi_{\mu_n}$ . (3.55)

Multiplying (3.53) by  $\nabla \overline{\psi}_{\mu_n}$ , integrating over  $Y \setminus R$ , and using the jump condition  $n \cdot \varepsilon_{p,\mathrm{rel}}(\omega_0)(\nabla w + \tilde{\mathbf{e}})|_{\partial P^-} = n \cdot (\nabla w + \tilde{\mathbf{e}})|_{\partial P^+}$ , we deduce that

$$a_{n} = -\tilde{\mathbf{e}} \cdot \frac{\int_{M} \nabla \overline{\psi}_{\mu_{n}} + \varepsilon_{p,\text{rel}}(\omega_{0}) \int_{P} \nabla \overline{\psi}_{\mu_{n}}}{1 - \mu_{n} + \varepsilon_{p,\text{rel}}(\omega_{0})\mu_{n}}.$$
(3.56)

In a similar way, from (3.54), we deduce that

$$b_{n} = -\frac{\int_{M} \nabla q \cdot \nabla \overline{\psi}_{\mu_{n}} + \varepsilon_{p,\text{rel}}(\omega_{0}) \int_{P} \nabla q \cdot \nabla \overline{\psi}_{\mu_{n}}}{1 - \mu_{n} + \varepsilon_{p,\text{rel}}(\omega_{0}) \mu_{n}}.$$
(3.57)

Using the orthogonality and substituting (3.52) and (3.55)–(3.57) into (3.26) with  $\tilde{\mathbf{v}}=\tilde{\mathbf{e}}$ , we obtain

$$\epsilon_{\text{eff}} \tilde{\mathbf{e}} \cdot \tilde{\mathbf{e}} = (\varepsilon_{p,\text{rel}}(\omega_0)\theta_P + \theta_M)\tilde{\mathbf{e}} \cdot \tilde{\mathbf{e}}$$

$$+ \theta_{Y \setminus R} \sum_{n=1}^{\infty} (1 + \mu_n(\varepsilon_{p,\text{rel}} - 1))(a_n + b_n)^2$$

$$+ \int_M \nabla q \cdot \nabla q + \varepsilon_{p,\text{rel}} \int_P \nabla q \cdot \nabla q.$$
(3.58)

And the proof of theorem 2.7 (2) is concluded.

# 4. Conclusion

The frequency-dependent effective dielectric permittivity and magnetic permeability are described by two types of subwavelength resonances: a plasmon resonance generating frequencydependent positive or negative effective dielectric properties and an artificial magnetic resonance generating a frequency-dependent effective magnetic permeability. In this article, we show how to employ these two resonances to rationally design double negative metamaterials. We numerically calculate the effective properties for metamaterial crystals made from coated sphere geometries and identified frequency intervals in the near infrared-optical regime where the metamaterial exhibits double negative behaviour. The term double negative refers to simultaneously negative effective magnetic permeability and dielectric permittivity, implying that the propagation of energy is opposite to the direction of phase velocity. The dependence of the sign of the effective magnetic permeability and effective dielectric permittivity depends on frequency. Frequency intervals corresponding to band gaps as well as intervals of normal dispersion and double negative dispersion are controlled explicitly through the geometry as seen in the theory and numerical experiments. Here, phenomenological modelling is not used but instead all results follow directly the Maxwell system on substituting a power series representation of the solution and examining leading order behaviour. We expect similar rigorous arguments to show that the power series represents the solution in three dimensions and this is a project for future work.

Data accessibility. Source code and files of all computations are available at https://github.com/Adil-Abit/Controlling-the-Dispersion-of-Metamaterials-in-3-d.

Authors' contributions. A.A.: conceptualization, formal analysis, software, validation, visualization, writing—original draft, writing—review and editing; Y.C.: conceptualization, formal analysis, validation, visualization, writing—original draft; R.L.: conceptualization, formal analysis, supervision, validation, visualization, writing—original draft, writing—review and editing; S.W.: software, validation, visualization, writing—original draft.

All authors gave final approval for publication and agreed to be held accountable for the work performed therein.

Conflict of interest declaration. We declare we have no competing interests.

Funding. This research work is supported in part by NSF grant nos. DMS-1813698 and DMREF-1921707.

# References

Downloaded from https://royalsocietypublishing.org/ on 16 August 2022

- 1. Veselago VG. 1967 Electrodynamics of substances with simultaneously negative values of  $\epsilon$  and  $\mu$ . Usp. Fiz. Nauk 92, 517. (doi:10.3367/UFNr.0092.196707d.0517)
- Pendry JB, Holden AJ, Robbins DJ, Stewart WJ. 1999 Magnetism from conductors and enhanced nonlinear phenomena. *IEEE Trans. Microwave Theory Tech.* 47, 2075–2084. (doi:10.1109/22.798002)
- 3. Smith DR, Padilla WJ, Vier DC, Nemat-Nasser SC, Schultz S. 2000 Composite medium with simultaneously negative permeability and permittivity. *Phys. Rev. Lett.* **84**, 4184–4187. (doi:10.1103/PhysRevLett.84.4184)
- Zhang F, Potet S, Carbonell J, Lheurette E, Vanbesien O, Zhao X, Lippens D. 2008 Negativezero-positive refractive index in a prism-like omega-type metamaterial. *IEEE Trans. Microwave Theory Tech.* 56, 2566–2573. (doi:10.1109/TMTT.2008.2005891)
- 5. Zhang S, Fan W, Minhas BK, Frauenglass A, Malloy KJ, Brueck SRJ. 2005 Midinfrared resonant magnetic nanostructures exhibiting a negative permeability. *Phys. Rev. Lett.* **94**, 037402. (doi:10.1103/PhysRevLett.94.037402)
- Zhou X, Zhao XP. 2007 Resonant condition of unitary dendritic structure with overlapping negative permittivity and permeability. *Appl. Phys. Lett.* 91, 181908. (doi:10.1063/1.279 8063)
- 8063)
  7. Huangfu J, Ran L, Chen H, Zhang X-m, Chen K, Grzegorczyk TM, Kong JA. 2004 Experimental confirmation of negative refractive index of a metamaterial composed of ω-like metallic patterns. *Appl. Phys. Lett.* **84**, 1537–1539. (doi:10.1063/1.1655673)

- 8. Dolling G, Enkrich C, Wegener M, Soukoulis CM, Linden S. 2006 Low-loss negative-index metamaterial at telecommunication wavelengths. *Opt. Lett.* **31**, 1800–1802. (doi:10.1364/OL.31.001800)
- Shalaev VM, Cai W, Chettiar UK, Yuan H-K, Sarychev AK, Drachev VP, Kildishev AV. 2005 Negative index of refraction in optical metamaterials. Opt. Lett. 30, 3356–3358. (doi:10.1364/ OL.30.003356)
- 10. Huang KC, Povinelli ML, Joannopoulos JD. 2004 Negative effective permeability in polaritonic photonic crystals. *Appl. Phys. Lett.* **85**, 543–545. (doi:10.1063/1.1775291)
- 11. Peng L, Ran L, Chen H, Zhang H, Kong JA, Grzegorczyk TM. 2007 Experimental observation of left-handed behavior in an array of standard dielectric resonators. *Phys. Rev. Lett.* **98**, 157403. (doi:10.1103/PhysRevLett.98.157403)
- 12. Vynck K, Felbacq D, Centeno E, Căbuz AI, Cassagne D, Guizal B. 2009 All-dielectric rod-type metamaterials at optical frequencies. *Phys. Rev. Lett.* **102**, 133901. (doi:10.1103/PhysRevLett.102.133901)
- 13. Wheeler MS, Aitchison JS, Mojahedi M. 2006 Coated nonmagnetic spheres with a negative index of refraction at infrared frequencies. *Phys. Rev. B* 73, 045105. (doi:10.1103/PhysRevB.73.045105)
- 14. Yannopapas V. 2007 Artificial magnetism and negative refractive index in three-dimensional metamaterials of spherical particles at near-infrared and visible frequencies. *Appl. Phys. A* 87, 259–264. (doi:10.1007/s00339-006-3815-6)
- 15. Yannopapas V. 2007 Negative refractive index in the near-UV from Au-coated CuCl nanoparticle superlattices. *Phys. Status Solidi (RRL) Rapid Res. Lett.* **1**, 208–210. (doi:10.1002/pssr.200701191)
- 16. Chen Y, Lipton R. 2013 Multiscale methods for engineering double negative metamaterials. *Photonics Nanostruct. Fundam. Appl.* **11**, 442–452. (doi:10.1016/j.photonics.2013.07.005)
- 17. Chen Y, Lipton R. 2013 Resonance and double negative behavior in metamaterials. *Arch. Ration. Mech. Anal.* 209, 835–868. (doi:10.1007/s00205-013-0634-8)
- 18. Shvets G, Urzhumov YA. 2004 Engineering the electromagnetic properties of periodic nanostructures using electrostatic resonances. *Phys. Rev. Lett.* **93**, 243902. (doi:10.1103/PhysRevLett.93.243902)
- 19. Alù A, Engheta N. 2008 Dynamical theory of artificial optical magnetism produced by rings of plasmonic nanoparticles. *Phys. Rev. B* **78**, 085112. (doi:10.1103/PhysRevB.78.085112)
- Fortes SP, Lipton RP, Shipman SP. 2010 Sub-wavelength plasmonic crystals: dispersion relations and effective properties. *Proc. R. Soc. A* 466, 1993–2020. (doi:10.1098/rspa.2009. 0542)
- 21. Fortes SP, Lipton RP, Shipman SP. 2011 Convergent power series for fields in positive or negative high-contrast periodic media. *Commun. Partial Differ. Equ.* **36**, 1016–1043. (doi:10.1080/03605302.2010.531860)
- 22. Shipman SP. 2010 Power series for waves in micro-resonator arrays. In 2010 Int. Conf. on Mathematical Methods in Electromagnetic Theory, Kyiv, Ukraine, 6–8 September 2010. (doi:10.1109/MMET.2010.5611403)
- 23. Chen Y, Lipton R. 2018 Controlling refraction using sub-wavelength resonators. *Appl. Sci.* **8**, 1942. (doi:10.3390/app8101942)
- 24. Bouchitté G, Bourel C, Felbacq D. 2017 Homogenization near resonances and artificial magnetism in three dimensional dielectric metamaterials. *Arch. Ration. Mech. Anal.* 225, 1233–1277. (doi:10.1007/s00205-017-1132-1)
- 25. Lipton R, Schweizer B. 2018 Effective Maxwell's equations for perfectly conducting split ring resonators. *Arch. Ration. Mech. Anal.* **229**, 1197–1221. (doi:10.1007/s00205-018-1237-1)
- Lamacz A, Schweizer B. 2016 A negative index meta-material for Maxwell's equations. SIAM J. Math. Anal. 48, 4155–4174. (doi:10.1137/16M1064246)
- 27. Lipton R, Viator R, Bolanos J, Adili A. 2021 Bloch waves in high contrast electromagnetic crystals. (http://arxiv.org/abs/2110.12262v1)
- 28. Bergman DJ. 1978 The dielectric constant of a composite material: a problem in classical physics. *Phys. Rep.* 43, 377–407. (doi:10.1016/0370-1573(78)90009-1)
- 29. McPhedran RC, Milton GW. 1981 Bounds and exact theories for transport properties of inhomogeneous media. *Appl. Phys. A* 26, 207–220. (doi:10.1007/BF00617840)
- 30. Mayergoyz I, Fredkin D, Zhang Z. 2005 Electrostatic (plasmon) resonances in nanoparticles. *Phys. Rev. B* **72**, 155412. (doi:10.1103/PhysRevB.72.155412)

royalsocietypublishing.org/journal/rspa Proc. R. Soc. A 478: 20220194

- 31. Poelstra KH, Schweizer B, Urban M. 2021 The geometric average of curl-free fields in periodic geometries. *Analysis* **41**, 179–197. (doi:10.1515/anly-2020-0053)
- 32. Bouchitté G, Schweizer B. 2010 Homogenization of Maxwell's equations in a split ring geometry. *Multiscale Model. Simul.* **8**, 717–750. (doi:10.1137/09074557X)
- 33. Walker SW. 2018 Felicity: a MATLAB/C++ toolbox for developing finite element methods and simulation modeling. *SIAM J. Sci. Comput.* **40**, C234–C257. (doi:10.1137/17M11 28745)